Measuring absolute microvascular blood flow in cortex using visible-light optical coherence tomography

Siyu Chen, Ji Yi, Sam Inayat, Wenzhong Liu, Jianhua Cang, and Hao F. Zhang

***Abstract*—Understanding regulating mechanisms of cerebral blood flow (CBF) is important for clinical diagnosis and biomedical researches. We demonstrate here that phase sensitive Doppler optical coherence tomography is able to measure absolute CBF in mouse visual cortex *in vivo* when working in the visible-light spectral range. Both temporal and spatial profile of regional CBF variations can be resolved. We further assessed the accuracy of our method by *in vitro* experiments, which showed great consistency between the measured values and controlled ones. Finally, we enhanced the contrast of blood vessels to generate an angiogram showing great details of mouse cortical microvasculature.**

I. Introduction

Cerebral circulation delivers oxygenated blood to the brain and removes deoxygenated blood as well as wastes. Cerebral blood flow (CBF) is tightly regulated to satisfy the high energy demands of neurons. Abnormal alterations in CBF may indicate a pathological change in brain, whose complications include hypertension, Alzheimer's disease, and ischemic strokes [1]. Early medical intervention is a necessity for promising treatment of these diseases [2,3]. Therefore, quantitative monitoring of CBF serves as an important indicator for diagnosis and prognosis in clinical settings. Furthermore, the coupling between local CBF and oxygen metabolism during neural activation provides researchers an indirect method to measure the regional brain neuron activities [4]. The information gives an insight of the functionality of cortical neuron networks and leads to better understandings of the brain.

Despite the importance, it is still challenging to achieve real-time, high resolution monitoring of absolute CBF *in vivo*. Currently, major clinical-accessible approaches include functional magnetic resonance imaging (fMRI) and positron emission tomography (PET). Both techniques can provide three dimensional *in vivo* mapping of blood flow non-invasively. However, the spatial and temporal resolution is limited and sometimes requires the use of chemical or radioactive labels [5,6].

Resrach supported by the NIH grants 1R01EY019951 and 1R24EY022883. NSF grant CBET-1055379.

Siyu Chen, Ji Yi, and Wenzhong Liu are with the Biomedical Engineering Department, Northwestern University, Evanston, Illinois, 60208, USA. (e-mail: siyuchen2012@u.northwestern.edu).

Sam Inayat and Jianhua Cang are with the Neurobiology Department, Northwestern University, Evanston, Illinois, 60208, USA.

Hao F. Zhang is with the Biomedical Engineering Department, Northwestern University Evanston, Illinois, 60208, USA, as well as the Ophthalmology Department, Northwestern University, Chicago, IL 60611, USA (phone: 847-491-2946; fax: 847-491-4928; e-mail: hfzhang@northwestern.edu)

Other approaches include scanning laser Doppler and laser speckle imaging [7]. Scanning laser Doppler measures the projected velocity along the probing beam axis based on the Doppler frequency shift caused by moving optically scattering particles [8]. However, the absolute value cannot be easily recovered without knowing the Doppler angle due to lack of depth information. For laser speckle imaging, the spatial and temporal speckle pattern is used to extract cerebral blood [9]. However, confounding factors, including dimensions and numbers of the particle and geometry of the optical system, make determine of absolution particle velocity very challenging [10].

Recently, several research groups have demonstrated the feasibility of phase sensitive Doppler optical coherence tomography (DOCT) for flow measurement both in vitro and in vivo [11-14]. The advantage of DOCT is that three-dimensional volumetric information can be obtained simultaneously. The volumetric data allow us to obtain orientation of the blood vessels as well as the projected velocity, which enables the calculation of absolute blood velocity and flow.

While currently the majority of DOCT systems use near infrared (NIR) illumination source, visible-light OCT begin to emerge [15]. Using shorter wavelengths, visible-light OCT system offers twice as good axial resolution. Furthermore, the visible spectral range is where the optical properties of oxyhemoglobin and deoxyhemoglobin maintain the greatest contrast [16]. This allows the extraction of blood oxygen saturation (sO_2) from OCT spectral analysis. Both *in vitro* and i*n vivo* experiments have been reported to determine blood sO_2 with high accuracy and consistency [17,18].

We demonstrated here that we can achieve quantitative CBF measurement using visible-light DOCT (vis-DOCT) in the mouse cortex. The accuracy of vis-DOCT was confirmed by *in vitro* experiments. We also incorporated statistical modeling to enhance the contrast of microvasculature to generate comprehensive angiography of mouse cortex.

II. Methods and Materials

A. Animal preparation

The mouse was first anesthetized by intraperitoneal injection of urethane (1.2 – 1.3 g/kg in 10% saline solution). We waited 10 minutes to allow the mouse to enter the desired stable anesthesia plane and then placed it on a stereotaxic apparatus. During the experiment, we monitored and maintained the mouse core temperature at 37 °C by a small animal heating pad with feedback control. Artificial

tear was applied on both eyes every other minute to prevent dehydration.

A small craniotomy was performed at the left hemisphere to expose the visual cortex for imaging. The area of the incision is about 1.5 mm in diameter. After the surgery, the mouse was allowed 10 minutes to recover and then transferred to the imaging apparatus. During the imaging process, the animal was maintained in deep anesthesia state and inhaled pure oxygen. All animal experimental procedures were approved by the Institutional Animal Care and Use Committee at Northwestern University.

B. *vis-DOCT imaging of mouse visual cortex*

A house-built, free-space vis-DOCT system was used to image the mouse brain cortex (Fig. 1(a)). A supercontinuum laser source provided the illumination light covering 512 nm to 620 nm, which corresponded to an axial resolution of 1.3 μm in air. The illumination light was split into the sample arm and reference arm by a 50:50 beam splitter. A pair of galvanometer mirrors scanned the sample beam to cover an sample area of 1.5 mm by 1.5 mm through a scanning objective lens (f = 39 mm). The recombined interference spectrum was then sampled by a home-made spectrometer. For data processing, we first resampled and interpolated the acquired spectrum to be equal interval in *k*-space. A fast Fourier transform was then performed to recover the auto-correlation function of the illumination light. The OCT amplitude and phase image were recovered from the modulus and argument of the auto-correlation function, respectively.

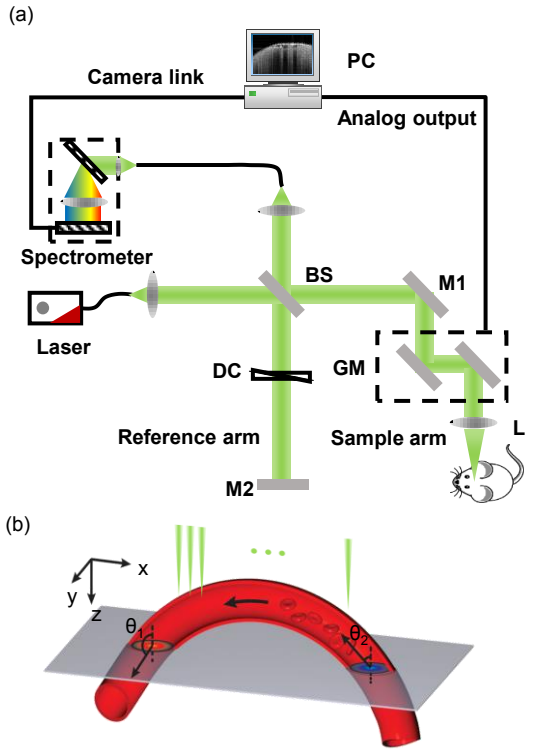

Figure 1. Schematic diagram of visible vis-DOCT. (a) System configuration. BS: beam splitter; M1, M2: mirror; GM: galvanometer mirrors; L: objective lens; DC: dispersion control. (b) Measuring absolute CBF on C-plane.

C. *vis-DOCT CBF measurement*

We used phase sensitive Doppler OCT for CBF measurement [11]. Two scanning protocols were incorporated to investigate the temporal and spatial profile of mouse CBF, respectively. For temporal CBF, we monitored blood flow velocity at one specific blood vessel cross-section over 5 seconds by repetitively acquiring B-scans at 12 frames per second. We calculated the blood flow velocity extracted from each frame. The projected velocity v [m/s] along the beam axis is

$$v = \frac{f_{sample} \cdot \lambda_c \cdot \Delta\varphi}{4 \cdot \pi \cdot n}, \quad (1)$$

where f_{sample} [Hz] is the sampling frequency of A-line; λ_c [m] is the center wavelength; $\Delta\varphi$ [radian] is the velocity induced phase shift; and n [dimensionless] is the refractive index of cortical tissue.

To acquire the absolute CBF and its spatial distribution, a two-dimensional raster scan on the exposed cortex area was performed. We then measured the vessel diameter and orientation of the blood vessel from the volumetric structural OCT image. The blood flow is then calculated as

$$F = u \cdot A = \frac{v}{\cos(\theta)} \cdot \frac{\pi \cdot d^2}{4}, \quad (2)$$

where u [m/s] is the mean absolute blood velocity; θ [radian] is the Doppler angle between the probing laser axis and the actual direction of blood velocity; d [m] is the vessel diameter.

After re-arranging (2) as (3), we found that the absolute flow can be calculated by integrating velocity within the cross-section of vessel in x-y plane (C-plane).

$$F = v \cdot \frac{\pi \cdot d^2}{4 \cdot \cos(\theta)} = v \cdot A_{x-y}, \quad (3)$$

where $A_{x\text{-}y}$ is the projected vessel cross-section in the C-plane. $A_{x\text{-}y}$ can be readily obtained by examine the OCT C-plane image containing blood vessels as demonstrated in Fig. 1(b). The method allows us to obtain absolute CBF without explicitly calculate the Doppler angle, which facilitate the process and minimize calculating errors [14].

D. *Cortex angiography*

We generated cortex angiography from the volumetric OCT phase image acquired. We observed that the velocity-encoded OCT phase image showed little variation for solid tissues. However, the phase values showed strong random distribution due to particle movements in blood vessels. The same phenomenon was also observed by other groups and can be explained by scattering speckle caused by stationary and moving particles [14]. We enhanced the contrast of blood vessels taking advantage of strong phase variation inside blood vessels. Specifically, image segmentation was firstly performed to eliminate background noise. A standard deviation (STD) filter (3 by 3 in size) was then performed in each C-plane to enhance the contrast of the blood vessels. After STD filtering, we projected the mean intensity to along the depth axis to generate a two-dimensional angiogram on C-plane showing the cortical microvasculature.

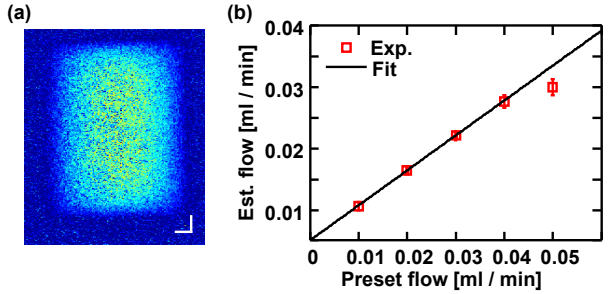

Figure 2. Verification of vis-DOCT flow meter. (a) OCT phase image of one selected C-plane. (b) Linear regression of estimated flow. Scale bar: 50 µm.

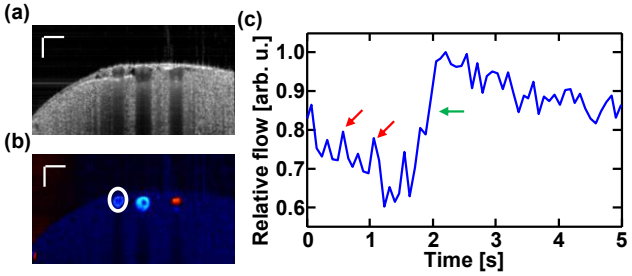

Figure 3. Mouse cortex cross-section generated by visible light DOCT. (a) Structural B-Scan image of the mouse cortex. (b) Phase encoded DOCT cross-section. (c) Relative flow change of the blood vessel shown in (b). Scale bar: 100 µm. Red arrows indicate CBF fluctuation caused by heart beats. Green arrow indicates CBF fluctuation caused by respiration.

III. RESULTS

A. vis-DOCT flow measurement in vitro

We assess the accuracy of vis-DOCT flowmetry by constructing and imaging a straight micro-channel filled with 1% Intralipid. The channel is 500 µm wide and 150 µm high, with the fluid inside driven by a syringe pump at a rate from 0.01 ml/min to 0.05 ml/min. We tilted the sample about 30 degrees to allow absolute flow to be calculated from C-plane images using the method describe above. Fig. 2(a) shows OCT phase image of one C-plane.

For each infusion rate, ten consecutive C-plane images containing complete micro-channel structure were empirically chosen. Within each C-plane image, we calculated the absolute flow independently. The mean and standard deviation of the calculated flow are plot against increasing preset infusion rate in Fig. 2(b). The measured flow showed strong linear correlation with preset flow when flow rate is less than 0.04 ml/min. However, when the flow rate approached 0.05 ml/min, the measured value was lower than expected. A close examination on the OCT phase image showed appearance of random phase wrap caused by high flow velocity, which accounts for underestimation.

We performed a regression analysis on the first four data point, and the results showed strong linear correlation (R^2 = 0.9998) between the preset and measured flow:

$$y = 0.57 \cdot x + 0.005 \quad , \tag{4}$$

where x and y represents preset and measured flow, respectively. Thus, a scaling factor of 0.57 was used to scale the *in vivo* flow measurement data for calibration. The reason why a coefficient of 0.57 rather than 1 was used can be explained by the de-noising process performed to obtain the OCT phase image. The de-noising algorithm averaged out extreme phase values as well as random noise, which underestimates the absolute flow.

B. vis-DOCT measurement of temporal CBF profile

We monitored blood velocity of a single vessel over multiple cardiac cycles. Fig. 3(a) and (b) show the OCT amplitude and phase image of the selected blood vessel and surrounding tissues, respectively. We calculated the relative blood velocity across the cross-section using the method described above, and the measured relative velocity was plotted against time in Fig. 3(c). A Fourier analysis was performed, showing a peak frequency of 4.1 Hz besides the DC component. The value corresponded to the physiological findings of heart rate of deeply anesthetized mouse. Moreover, we believed that the elevation in the middle of the curve is caused by respiration, with its frequency also matches the breath frequency of mouse.

C. vis-DOCT measurement of spatial CBF profile

We calculated the absolute CBF at five different C planes. The depth location of each plane is illustrated in Fig. 4(a). As we can see, there was at least one of the major cortical blood vessels within each C plane. The corresponding slices were shown in Fig. 4(b) to (f), The red and blue color indicates the flow directions relative to probing beam, with blue indicates a flow velocity towards the probing laser and red away from the laser. We observed red and blue interleave within one vessel, which indicates change of blood flow direction, and this was confirmed by wavy propagation of cortical blood vessels found in volumetric OCT amplitude image. The findings also agrees with earlier studies on CBF by other groups [14].

We calculated the absolute CBF from sapling locations indicated by "X" in Fig. 4. The calculated CBF values are listed in table 1.

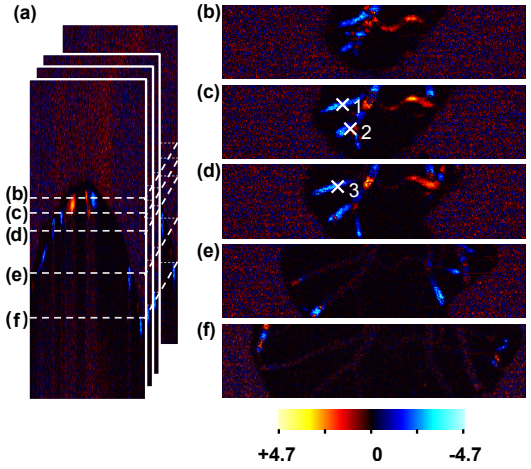

Figure 4. vis-DOCT flow measurement. (a) vis-DOCT phase image of B-scans arranged in stacks showing the C-planes where flow measurements are taken. (b) to (f) Velocity mapping of C-planes indicated in (a). Color bar: projected velocity [mm / s], positive values indicate flow direction away from the probing laser.

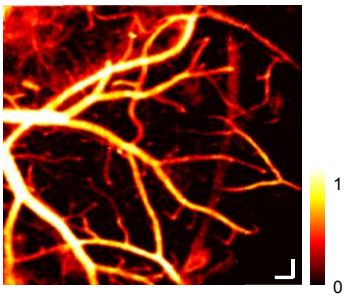

Figure 5. Enhanced angiogram showing blood vasculature of mouse cortex. Scale bar: 100 μm.

The sampling position 1 and 2 are the cross-section of the same blood vessel in different C-planes. The absolute CBF calculated agree with each other for these two sample points.

TABLE 1 ABSOLUTE CBF MEASURED AT SELECTED POSITION

Locations:	CBF [$\times 10^{-8}$ L/min]
1	2.33
2	1.95
3	2.17

D. Mouse Cortex angiography

We employed the aforementioned statistical analysis to enhance the contrast of small blood vessels which are not readily seen under normal OCT amplitude images. Using the same data sets as which were used for CBF measurement, we acquired the high-resolution cortex angiogram covering an area of 1.8 mm by 1.8 mm (Figure 5). The intensity of the graph indicates the local randomness of the OCT phase image. As can be seen from the figure, larger vessel shows the highest intensity due to faster flow and thus greater phase variation. Smaller vessels are also much enhanced. Most importantly, static backgrounds are suppressed and rendered as pure black in the generated the angiogram. This provides maximum imaging contrast to the microvasculature imaged.

IV. DISCUSSION AND CONCLUSION

In the presented study, we demonstrated the capability of vis-DOCT to measure absolute blood flow in mouse cortex. Both temporal and spatial variation of cortex CBF can be resolved. Further, a phantom experiment was conducted to investigate the accuracy of vis-DOCT flow measurement. The measured values showed great consistency against the preset ones within a constant scaling factor for small flow rates. Finally, an enhanced angiogram was generated to show the high-resolution imaging capability of cortical microvasculature using our vis-DOCT system.

One advantage of vis-DOCT is its capability of extracting blood oxygen saturation using intrinsic optical contrast of oxyhemoglobin and deoxyhemoglobin. Combined with absolute blood flow measurement, it is straightforward to calculate the oxygen consumption of local tissue. The technique further allows in vivo measurement of local cell metabolism and activity.

Despite the merits, there are still limits need to be overcame. We found that the unscaled measured flow is merely over half of the actual value as revealed in the in vitro experiment. A scaling coefficient must be incorporated to compensate for the discrepancy. Further investigations suggested that the de-noising process we performed was responsible for the difference. Thus, a better imaging processing techniques that can both preserve the extreme values as well as effectively remove random noise is required.

REFERENCES

[1] H. Girouard and C. Iadecola, "Neurovascular coupling in the normal brain and in hypertension, stroke, and Alzheimer disease," *J. Appl. Physiol.*, vol. 100, pp. 328-335, Jan. 2006.

[2] J. L. Cummings, R. Doody, and C. Clark, "Disease-modifying therapies for Alzheimer disease challenges to early intervention," *Neurology*, vol. 69, pp. 1622-1634, 2007.

[3] S. H. Hayes and S. R. Carroll, "Early intervention care in the acute stroke patient," *Arch. Phys. Med. Rehabil.*, vol. 67, pp. 319-321, May 1986.

[4] M. Jueptner and C. Weiller, "Review: Does measurement of regional cerebral blood flow reflect synaptic activity? - Implications for PET and fMRI," *NeuroImage*, vol. 2, pp. 148-156, Jun. 1995.

[5] F. Calamante, D. L. Thomas, G. S. Pell, J. Wiersma, and R. Turner, "Measuring cerebral blood flow using magnetic resonance imaging techniques," *J. Cereb. Blood Flow Metab.*, vol. 19, pp. 701-735, Jul. 1999.

[6] K. J. Friston, C. D. Frith, P. F. Liddle, and R. S. J. Frackowiak, "Comparing functional (PET) images: the assessment of significant change," *J. Cereb. Blood Flow Metab.*, vol. 11, pp. 690-699, Jan. 1991.

[7] J. D. Briers, "Laser Doppler, speckle and related techniques for blood perfusion mapping and imaging," *Physiol. Meas.*, vol. 22, pp. R35, 2001.

[8] M. Jones, J. Berwick, D. Johnston, and J. Mayhew, "Concurrent optical imaging spectroscopy and Laser-Doppler flowmetry: The relationship between blood flow, oxygenation, and volume in rodent barrel cortex," *NeuroImage*, vol. 13, pp. Jun. 2001.

[9] A. K. Dunn, H. Bolay, M. A. Moskowitz, and D. A. Boas, "Dynamic imaging of cerebral blood flow using laser speckle," *J. Cereb. Blood Flow Metab.*, vol. 21, pp. 195-201, Mar. 2001.

[10] D. A. Boas and A. K. Dunn, "Laser speckle contrast imaging in biomedical optics," *J. Biomed. Opt.*, vol. 15, pp. 011109-12, 2010.

[11] J. A. Izatt, M. D. Kulkarni, S. Yazdanfar, J. K. Barton, and A. J. Welch, "*In vivo* bidirectional color Doppler flow imaging of picoliter blood volumes using optical coherence tomography," *Opt. Lett.*, vol. 22, pp. 1439-1441, Sep. 1997.

[12] J. M. Schmitt, "Optical coherence tomography (OCT): a review," *IEEE J. Sel. Top. Quant.*, vol. 5, pp. 1205-1215, 1999.

[13] R. A. Leitgeb, L. Schmetterer, C. K. Hitzenberger, A. F. Fercher, F. Berisha, M. Wojtkowski, et al., "Real-time measurement of *in vitro* flow by Fourier-domain color Doppler optical coherence tomography," *Opt. Lett.*, vol. 29, pp. 171-173, May 2004.

[14] V. J. Srinivasan, S. Sakadžić, I. Gorczynska, S. Ruvinskaya, W. Wu, J. G. Fujimoto, and D. A. Boas, "Quantitative cerebral blood flow with Optical Coherence Tomography," *Opt. Expr.*, vol. 18, pp. 2477-2494, Feb. 2010.

[15] X. Zhang, J. Hu, R. W. Knighton, X.-R. Huang, C. A. Puliafito, and S. Jiao, "Visible light optical coherence tomography for in vivo imaging the spectral contrasts of the retinal nerve fiber layer," *Proc. SPIE*, pp. 82130H-82130H-7, 2012.

[16] N. Bosschaart, G. Edelman, M. G. Aalders, T. Leeuwen, and D. Faber, "A literature review and novel theoretical approach on the optical properties of whole blood," *Laser. Med.*, vol. 29, pp. 453-479, Mar. 2014.

[17] J. Yi and X. Li, "Estimation of oxygen saturation from erythrocytes by high-resolution spectroscopic optical coherence tomography," *Opt. Lett.*, vol. 35, pp. 2094-2096, Jun. 2010.

[18] J. Yi, Q. Wei, W. Liu, V. Backman, and H. F. Zhang, "Visible-light optical coherence tomography for retinal oximetry," *Opt. Lett.*, vol. 38, pp. 1796-1798, Jun. 2013.